

- Sci.* **1982**, *86*, 476.
2. Messinger, B. J.; von Raben, K. U.; Chang, R. K.; Barber, P. W. *Phys. Rev. B.* **1981**, *24*, 649.
  3. Change, R. K.; Furtak, T. E., eds. *Surface Enhanced Raman Scattering*; Plenum Press: New York, 1982.
  4. Hayashi, S.; Koh, R.; Ichuyama, Y.; Yamamoto, K. *Phys. Rev. Lett.* **1988**, *60*, 1085.
  5. Wang, Y. *J. Phys. Chem.* **1991**, *95*, 1119.
  6. Kerker, M. *The Scattering of Light and Other Electromagnetic Radiation*; Academic Press: New York, 1969.
  7. Wiscombe, W. J. *Document PB 301388*; National Technical Information Service: Springfield, VA, 1979.
  8. Madelung, O., Ed., *Landolt-Bornstein, New Series, Vol. 17 b*; Springer Verlag: New York, 1983.
  9. Benincasa, D. S.; Barber, P. W.; Zhang, J.-Z.; Hsieh, W.-F.; Chang, R. K. *Appl. Opt.* **1987**, *26*, 1348.
  10. Ching, S. C.; Lai, H. M.; Young, K. *J. Opt. Soc. Am. B*, **1987**, *4*, 1995; **1987**, *4*, 2004.
  11. Hill, S. C.; Benner, R. E. *J. Opt. Soc. Am. B* **1986**, *3*, 1509.
  12. Tzeng, H.-M.; Wall, K. F.; Long, M. B.; Chang, R. K. *Opt. Lett.* **1984**, *9*, 499.
  13. Campillo, A. J.; Eversole, J. D.; Lin, H.-B. *Phys. Rev. Lett.* **1991**, *67*, 437.
  14. Lam, C. C.; Leung, P. T.; Young, K. *J. Opt. Soc. Am. B*, **1992**, *9*, 1585.
  15. Chylek, P. *J. Opt. Soc. Am.* **1976**, *66*, 285.
  16. Chylek, P.; Lin, H.-B.; Eversole, J. D.; Campillo, A. J. *Opt. Lett.* **1991**, *16*, 1723.
  17. Lin, H.-B.; Huston, A. L.; Eversole, J. D.; Campillo, A. J.; Chylek, P. *Opt. Lett.* **1992**, *17*, 970.
  18. Lin, H.-B.; Campillo, A. J. *Appl. Opt.* **1985**, *24*, 422.
  19. Benner, R. E.; Barber, P. W.; Owen, J. F.; Chang, R. K. *Phys. Rev. Lett.* **1980**, *44*, 475.
  20. Thurn, R.; Kiefer, W. *Appl. Opt.* **1985**, *24*, 1515.

## Scattering of Noble Gas Ions from a Si(100) Surface at Hyperthermal Energies (20-300 eV)

Hyun-Woo Lee and H. Kang\*

*Department of Chemistry, Pohang University of Science and Technology, Pohang, Gyeong-buk 790-784, Korea*

*Received September 1, 1994*

In an attempt to understand the nature of hyperthermal ion-surface collisions, noble gas ion beams ( $\text{He}^+$ ,  $\text{Ne}^+$ ,  $\text{Ar}^+$ , and  $\text{Xe}^+$ ) are scattered from a Si(100) surface for collision energies of 20-300 eV and for  $45^\circ$  incidence angle. The scattered ions are mass-analyzed using a quadrupole mass spectrometer and their kinetic energy is measured in a time-of-flight mode. The scattering event for  $\text{He}^+$  and  $\text{Ne}^+$  can be approximated as a sequence of quasi-binary collisions with individual Si atoms for high collision energies ( $E_i > 100$  eV), but it becomes of a many-body nature for lower energies,  $\text{Ar}^+$  and  $\text{Xe}^+$  ions undergo multiple large impact parameter collisions with the surface atoms. The effective mass of a surface that these heavy ions experience during the collision increases drastically for low beam energies.

### Introduction

Knowledge of the nature of gas-surface collision is important for the processes of adsorption, film deposition, etching, and chemical reactions. Gas-surface scattering technique has been extensively employed for last 20 years in order to obtain information about the collisional nature.<sup>1,2</sup> While these investigations have made significant advances for our understanding of gas-surface collisions, one also becomes realized of a diverse nature of this subject and we are only at the beginning stage of exploration. Depending on collision energy, the nature of scattering can vary from thermal ( $< 1$  eV) to binary events (keV). The terminology "hyperthermal" refers to the energy range in which transition between the two

different regimes occurs.

Recently, several research groups have explored hyperthermal gas-surface scattering using supersonic atomic beams<sup>3,4</sup> and ion beams.<sup>5-10</sup> In most of these works the mass of a projectile is smaller than a surface atom. The studies of heavy projectile-surface collision is very rare.<sup>3,10</sup> With supersonic beams the collisional energy that can be investigated is limited usually below 10 eV. While ion beams can access to a higher energy, ion scattering has not been widely employed because hyperthermal ion beams are instrumentally difficult to handle and these ions become efficiently neutralized upon surface collisions. In the present work, we have examined the scattering behavior of noble gas ions from a Si surface over a substantially wide range of projectile mass ( $\text{He}^+$ ,  $\text{Ne}^+$ ,  $\text{Ar}^+$ , and  $\text{Xe}^+$ ) and collision energy (20-300 eV). Such a study enables us to explore the effects of projectile mass and energy on the scattering nature. We find from this study that the heavier ions ( $\text{Ar}^+$  and  $\text{Xe}^+$ ) scatter from

\*To whom correspondence should be addressed.

This paper is dedicated to Professor Woon-Sun Ahn in honor of his retirement.

surface as a result of extensive multiple collisions while the lighter ions ( $\text{He}^+$  and  $\text{Ne}^+$ ) undergo quasi-single or double collisions with surface atoms at relatively high energies.

### Experimental Section

The experiment was carried out in an ion-surface collision chamber, which has been described in detail elsewhere.<sup>11,12</sup> The instrument consists of an ion beamline and an ultrahigh vacuum (UHV) surface analysis chamber. The beamline is designed to enhance low-energy performance, and differentially pumped at four stages in order to maintain UHV condition ( $2 \times 10^{-9}$  Torr) in the analysis chamber during the experiment.  $\text{He}^+$ ,  $\text{Ne}^+$ ,  $\text{Ar}^+$ , and  $\text{Xe}^+$  ions were generated by electron impact ionization of the noble gases. The ion beam was mass and energy-selected, and then bombarded onto a Si(100) target at the energies of 20-300 eV. The energy spread of a beam was normally less than 2 eV FWHM. In order to remove alkali ion impurities that are possibly contained in the beam of similar mass (eg.,  $\text{K}^+$  in  $\text{Ar}^+$  beam), the source was cleaned with a special care. A clean Si(100) surface was generated *in situ* by several cycles of 2 keV  $\text{Ar}^+$  sputtering and annealing at 1000 °C using electron bombardment from the back side. Surface impurity levels were below 1% of monolayer as checked by Auger electron spectroscopy.

Ions scattered from surface were mass-analyzed using a quadrupole mass spectrometer, and at the same time their kinetic energy was measured in a time-of-flight (TOF) mode. For TOF measurement the ion beam was electrically chopped into 1  $\mu\text{sec}$  pulses. The ion flight distance was 28 cm from a target to a detector. The angle between an incident beam and a detector was fixed at 90°, and the beam incidence direction was 45° to a target surface. TOF calibration was done using  $\text{He}^+$  and  $\text{Ne}^+$  beams scattered from a Ag surface, a combination for which a scattered particle energy can be accurately predicted from the classical binary collision (BC) model.<sup>13</sup> The calibration results matched well with the instrumental dimension.

### Results and Discussion

**$\text{He}^+$  and  $\text{Ne}^+$  scattering.** We first present scattering results for the ions lighter than a Si atom ( $\text{He}^+$  and  $\text{Ne}^+$ ). TOF spectra of  $\text{Ne}^+$  ions scattered from a Si(100) surface are shown in Figures 1(a) and (b) for 300 and 30 eV  $\text{Ne}^+$  beams, respectively. For ion incident energy ( $E_i$ ) of 300 eV, the scattered ions have an energy ( $E_s$ ) distribution which peaks at the position higher than that predicted for single 90° binary scattering from Si (marked by SS). A small hump is observed at the position corresponding to two successive 45° BC events with Si atoms (marked by DS). Most of the  $E_s$  distribution is encompassed by the SS and DS energies. At  $E_i$  of 30 eV the distribution shifts greatly toward the high energy side, and contains a very small population below the SS energy. The scattered ion yields are observed to be higher from Si surface than from metal surfaces (Cu and Ni) at least by one order, implying a lesser degree of ion neutralization on this semi-metallic surface (phosphorus-doped Si, resistivity = 10  $\Omega\text{cm}$ ).

The SS and DS positions of Figure 1 are calculated from

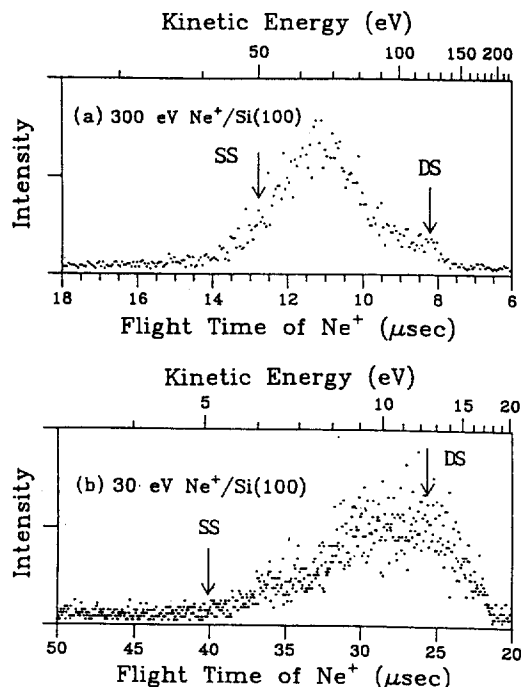


**Figure 1.** TOF spectra of  $\text{Ne}^+$  ions scattered from a Si(100) surface. The kinetic energy scale is also shown at the top of the figures. SS and DS represent the scattered energy positions corresponding to single and double BC events with Si atoms (see the text). The scattering angle is 90° with the beam incidence and exit angles of 45°. (a) 300 eV  $\text{Ne}^+$ . (b) 30 eV  $\text{Ne}^+$ .

the BC model (Eq. 1).<sup>14</sup>

$$\frac{E_s}{E_i} = \frac{1}{(1+A^2)} [\cos\Theta \pm (A^2 - \sin^2\Theta)^{1/2}]^2 \quad (1)$$

In this expression  $A = M_2/M_1$ , where  $M_1$  and  $M_2$  are the projectile and target atom masses, respectively, and  $\Theta$  is the laboratory scattering angle. The double sign applies to the case of heavier projectiles ( $A < 1$ ), and only the positive sign applies for the lighter ones ( $A \geq 1$ ). For heavier projectiles, which will be presented in the next section, the maximum binary scattering angle is  $\Theta_{\max} = \sin^{-1}A$ .

The energy of scattered ions is measured as a function of  $E_i$  in the range of 20-300 eV. The result is plotted in Figure 2 for  $\langle E_s \rangle / E_i$  vs  $E_i$ , where  $\langle E_s \rangle$  is the average scattered ion energy defined by Eq. 2

$$\langle E_s \rangle = \frac{\sum_j E_{sj} N_j}{\sum_j N_j} \quad (2)$$

$N_j$  represents the number of ions scattered with energy  $E_{sj}$ . With increasing  $E_i$ , the  $\langle E_s \rangle / E_i$  ratio decreases and approaches the SS value for a higher  $E_i$ . This approach is faster for  $\text{He}^+$  than for  $\text{Ne}^+$ , the second having a slightly higher  $\langle E_s \rangle$  than the SS energy even at  $E_i = 300$  eV. When  $E_i < 50$  eV, the  $\langle E_s \rangle / E_i$  ratio is much higher than the SS value, implying that BC approximation is no more valid.

Many-body collisional nature of the low energy ions is indicated from the following observations. First, the peak of  $E_s$  distribution is shifted from the SS position toward the

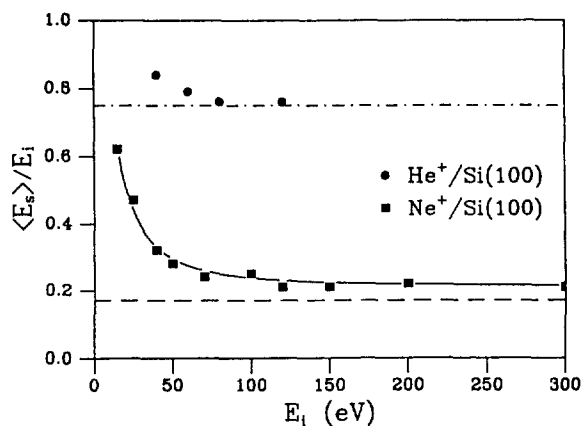


**Figure 2.** The ratio of the scattered to incident ion energy ( $\langle E_s \rangle / E_i$ ) plotted as a function of  $E_i$ . The single scattering value is indicated by the lines for He<sup>+</sup> (---) and Ne<sup>+</sup> (---).

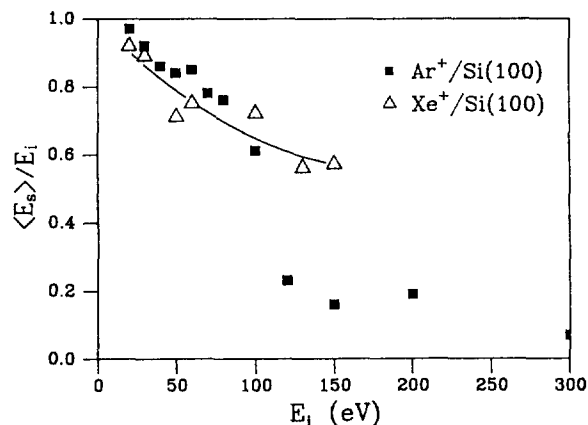


**Figure 3.** The ratio of the scattered to incident ion energy ( $\langle E_s \rangle / E_i$ ) plotted as a function of  $E_i$  for Ar<sup>+</sup> (■) and Xe<sup>+</sup> (△).

high  $E_s$  side (Figure 1). Such shift is distinct even at  $E_i$  of 300 eV, which we interpret as quasi-single scattering of the Ne<sup>+</sup> ion with a surface Si atom. Second, the features corresponding to the binary scattering peaks, *i.e.*, the SS and DS peaks, disappear in the TOF spectra of low  $E_i$ 's. These BC peaks are well resolvable in high energy (keV) experiments,<sup>15</sup> and in some cases, for lower energy experiments depending on a  $M_1/M_2$  combination, *eg.*, 600 eV Ne<sup>+</sup>-Ni(110),<sup>16</sup> 500 eV Ne<sup>+</sup>-Si(100),<sup>17</sup> and 40 eV He-Cu and 20 eV Ne<sup>+</sup>-Cu system.<sup>5</sup> In ref. 17 the SS and DS peaks are observed at slightly shifted positions from the BC values. Third, the deviation from the BC model is greater for Ne<sup>+</sup> than for He<sup>+</sup> and also for a lower  $E_i$  (Figure 2). Such mass and energy-dependences are confirmed by the molecular dynamics trajectory calculations of 10-500 eV noble gas atoms colliding with Ni(100) surface.<sup>18</sup>

**Ar<sup>+</sup> and Xe<sup>+</sup> scattering.** Due to their heavier masses than Si, binary scattering angles for Ar<sup>+</sup> and Xe<sup>+</sup> from Si are limited to 44.4° and 12.3°, respectively (Eq. 1). Thus, in our experimental geometry the scattered flux must originate from multiple scattering from the surface. Figure 3 presents the  $\langle E_s \rangle / E_i$  ratio for Ar<sup>+</sup> and Xe<sup>+</sup> ions scattered from the target as a function of  $E_i$ . The  $\langle E_s \rangle / E_i$  ratio is very high

in the lower energy region, approaching near unity (>0.9) at the lowest examined energy ( $E_i=20$  eV). The  $\langle E_s \rangle / E_i$  curve for Ar<sup>+</sup> decreases to a value of *ca.* 0.2 at  $E_i > 120$  eV. The Xe<sup>+</sup> data were not obtained above 150 eV because of extremely weak scattered ion signals.

An interesting aspect of the  $\langle E_s \rangle / E_i$  curves is that the heavy ions (Xe<sup>+</sup> and Ar<sup>+</sup>) scatter with a higher  $\langle E_s \rangle / E_i$  ratio than the light ions (He<sup>+</sup> and Ne<sup>+</sup>) for lower  $E_i$  collisions (<50 eV). This is possible only when the heavy ions scatter as a result of a large number of small angle deflections, while the light ions undergo less than a few, large angle deflections. For example, in order to retain 90% of initial energy after 90° scattering, Ar<sup>+</sup> has to make 30 successive binary collisions with Si atoms, each collision deflecting the Ar<sup>+</sup> trajectory by about 3° according to Eq. 2. For Xe<sup>+</sup>, about 100 collisions of 1° deflection are required. This argument is probably too simplified from the views that the BC approximation is not valid at this low energy and that the  $E_s$  distribution of low energy ions can be severely affected by ion neutralization factor. The effect of ion neutralization will be discussed further in the later section. Nevertheless, the high  $\langle E_s \rangle / E_i$  ratio for Xe<sup>+</sup> and Ar<sup>+</sup> is a clear indication of numerous collisions between the heavy particles and the surface atoms. Such multiple scattering trajectories are found to be characteristic to heavy projectile-surface collisions from molecular dynamics trajectory calculations.<sup>18</sup>

The  $\langle E_s \rangle / E_i$  value for Ar<sup>+</sup> decreases to 0.2 in the range of  $E_i=100-150$  eV. Such an energy retaining ratio implies that Ar<sup>+</sup> experiences 2-3 scattering events of 30-45° deflection with Si atoms according to the BC approximation. We also observed that Si substrate atoms started to be sputtered with a substantial rate above this energy. These observations suggest that above this energy Ar<sup>+</sup> ions start to interact with individual Si atoms and to penetrate the surface. The surface penetrated Ar<sup>+</sup> ions lose a great portion of initial energy during the collisions with many bulk atoms. However, since they are efficiently neutralized inside the solid, they will come out as neutral species and thus not be detected.

We can deduce the "effective mass" of a Si surface from the measured  $\langle E_s \rangle / E_i$  ratio. The effective mass is defined as the hypothetical surface mass that would give rise to an observed energy  $E_s$  after single 90° scattering event, and can be calculated from Eq. 1. Figure 4 shows the effective mass of the surface for Xe<sup>+</sup> and Ar<sup>+</sup> collisions in the units of the number of Si atoms. The effective mass greatly increases for low  $E_i$  collisions, reaching more than 50 Si atoms for  $E_i < 30$  eV. The effective mass is higher for a larger mass projectile. According to the classical trajectory analysis,<sup>18</sup> it seems quite unreasonable to assume that the projectile makes real collisional contacts with such a large number of Si atoms along its scattering trajectory. Rather, it is more likely that the Si atoms move in collective motions during the collision. Since the low energy Xe<sup>+</sup>-Si collision occurs in a relatively slow time scale ( $10^{-14}$ - $10^{-13}$  sec), the Si atoms near the impact site may also be pulled in, even without direct collisions with Xe<sup>+</sup>, *via* a vibrational relaxation process whose time scale is comparable to the collision time.

Experimental data for the  $\langle E_s \rangle / E_i$  ratio for heavy projectile-surface collisions are very scarce in the present  $E_i$  range.

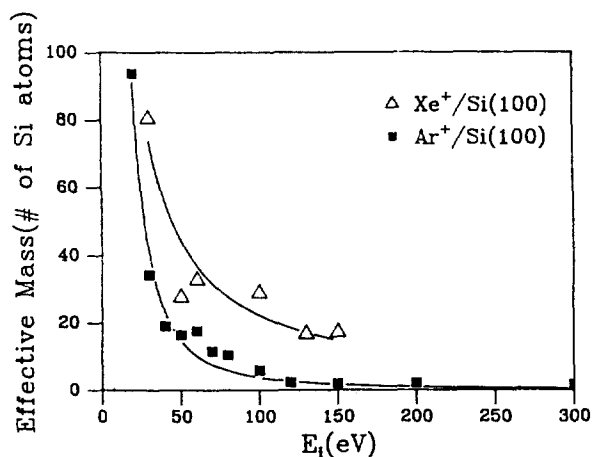


**Figure 4.** Variation in the effective mass of a Si surface as a function of  $E_i$  for  $\text{Ar}^+$  (■) and  $\text{Xe}^+$  (△) beams. Lines are drawn to guide the eye.

A molecular beam study of Hg-MgO(100) scattering has been reported,<sup>3</sup> in which an  $\langle E_s \rangle / E_i$  ratio of 0.56 was measured for a Hg beam of 8.7 eV with incidence and exit angles of  $21^\circ$  and  $24^\circ$  to a surface plane. Our  $\langle E_s \rangle / E_i$  value appears to be rather unusually high compared to this result, although such quantitative comparison may be only remotely possible due to the differences in the  $M_1/M_2$  ratio and in the scattering geometry. In addition, we need to take into account the neutralization factor of scattered ions in this comparison. When the ions deflect as a result of such soft, large impact parameter collisions, ion neutralization will occur mostly *via* resonant tunneling, which in turn, depends on collision time.<sup>19</sup> It is then very likely that the low  $E_s$  portion of the scattered flux is composed mostly of neutrals that do not appear in our spectrum. In this case the  $E_s$  distribution of ions will be located at the high energy side of the  $E_s$  distribution of the total scattered flux (both ions and neutrals). Thus, the present  $\langle E_s \rangle / E_i$  ratio may be interpreted as an upper limit of the total scattering events.

Finally, in order to examine the effect of ion neutralization we have recently performed a control experiment with  $\text{Cs}^+$  ions whose mass is similar to Xe. It is to be noted that  $\text{Cs}^+$  ions are not neutralized during scattering from Si surface, and thus the scattered ions truly represent the scattered flux. We observed from this experiment an  $\langle E_s \rangle / E_i$  curve qualitatively similar to the  $\text{Xe}^+$  result, but the absolute  $\langle E_s \rangle / E_i$  value was smaller for  $\text{Cs}^+$  scattering than for  $\text{Xe}^+$ . An  $\langle E_s \rangle / E_i$  value of 0.4 was observed at a  $\text{Cs}^+$  beam energy of 20 eV, and an  $\langle E_s \rangle / E_i$  value of 0.7 was reached at the energy as low as 5 eV. This indicates that ion neutralization does upshift the  $E_s$  distributions of scattered noble gas ions, but the qualitative features concerning the  $\langle E_s \rangle / E_i$  curve shape and the trend with projectile mass variation remain mostly valid.

### Conclusions

We have examined the scattering behavior of noble gas ions from Si(100) for 20-300 eV collisions. Multiple collisional nature is evident from the  $E_s$  distributions of these low ener-

gy ions. For  $\text{He}^-$  and  $\text{Ne}^+$ , the scattering process can be approximated as a sequence of quasi-binary collisions at  $E_i > 100$  eV. At lower energies, however, the BC peaks are no longer distinguishable in the TOF spectra and the scattering events become of a many-body nature.  $\text{Ar}^+$  and  $\text{Xe}^+$  always undergo many-body collisions with Si surface atoms, and the scattering occurs mostly *via* multiple, large impact parameter collisions with the surface Si atoms. As a result, the surface effective mass becomes very large for collisions of these low energy heavy ions.

The quantitative information about collision dynamics that can be drawn from the ionic  $E_s$  distribution is limited due to the ion neutralization factor. The present  $E_s$  values, and consequently the effective surface mass as well, may correspond to an upper limit of the neutral values. Despite such a limitation, the major qualitative conclusions stated in this section will remain valid, as indicated by the result of the control experiment using  $\text{Cs}^+$ .

**Acknowledgment.** We gratefully acknowledge the financial supports by KOSEF *via* Center for Molecular Science and the Ministry of Education of Korea (BSRI-94-3438).

### References

1. Goodman, F. O.; Wachman, H. Y. *Dynamics of Gas-surface Scattering*; Academic Press: New York, 1976.
2. Barker, J. A.; Auerbach, D. J. *Surf. Sci. Rep.* **1984**, *4*, 1.
3. Kolodney, E.; Amirav, A.; Elber, R.; Gerber, R. B. *Chem. Phys. Lett.* **1985**, *113*, 303.
4. Rettner, C. T.; Barker, J. A.; Bethune, D. S. *Phys. Rev. Lett.* **1991**, *67*, 2183.
5. Tongson, L. L.; Cooper, C. B.; *Surface Sci.* **1975**, *52*, 263.
6. Hulpke, E.; Mann, K. *Surface Sci.* **1983**, *133*, 171.
7. Tenner, A. D.; Gillen, K. T.; Horn, T. C. M.; Los, J.; Kleyn, A. W. *Phys. Rev. Lett.* **1984**, *52*, 2183.
8. McEachern, R. L.; Goodstein, D. M.; Cooper, B. H. *Phys. Rev. B* **1989**, *39*, 10503.
9. Snowdon, K. J.; O'connor, D. J.; MacDonald, R. J. *Surface Sci.* **1989**, *221*, 465.
10. Bazarbayev, N. N.; Evstifeev, V. V.; Krylov, N. M.; Kudryaschova, L. B. *Soviet J. Surface*, **1988**, *9*, 170.
11. Choi, W. Y.; Kang, T. H.; Kang, H. *Bull. Korean Chem. Soc.* **1990**, *11*, 290.
12. Park, K. H.; Kim, B. C.; Kang, K. *J. Chem. Phys.* **1992**, *97*, 2742.
13. Heiland, W.; Taglauer, E. *Instrum. Methods* **1976**, *132*, 535.
14. Smith, D. P. *J. Appl. Phys.* **1967**, *38*, 340.
15. Niehus, H.; Heiland, W.; Taglauer, E. *Surface Sci. Reports* **1993**, *17*, 1.
16. Taglauer, E.; Heiland, W. *Surface Sci.* **1972**, *33*, 27.
17. Murakami, J.; Hashimoto, T.; Kusunoki, I. *Vacuum* **1990**, *41*, 369.
18. Kim, C.; Kang, H.; Park, S. C. *Nucl. Instrum. Methods in Phys. Res. B* in press.
19. Hagstrum, H. D. *Inelastic Ion-Surface Collisions*; edited by N. H. Tolk *et al.*, p 1, Academic press: New York, 1977.